LASER INTERFEROMETER GRAVITATIONAL WAVE OBSERVATORY
- LIGO -
CALIFORNIA INSTITUTE OF TECHNOLOGY
MASSACHUSETTS INSTITUTE OF TECHNOLOGY

Technical Note **LIGO-T1800238–v1** 2018/11/15

Stabilization of a $2\mu m$ Laser using an all-fiber Delay Line Mach-Zehnder Interferometer

Vinicius Wagner

California Institute of Technology
LIGO Project, MS 18-34
Pasadena, CA 91125
Phone (626) 395-2129
Fax (626) 304-9834
E-mail: info@ligo.caltech.edu

Massachusetts Institute of Technology
LIGO Project, Room NW22-295
Cambridge, MA 02139
Phone (617) 253-4824
Fax (617) 253-7014
E-mail: info@ligo.mit.edu

LIGO Hanford Observatory
Route 10, Mile Marker 2
Richland, WA 99352
Phone (509) 372-8106
Fax (509) 372-8137
E-mail: info@ligo.caltech.edu

LIGO Livingston Observatory
19100 LIGO Lane
Livingston, LA 70754
Phone (225) 686-3100
Fax (225) 686-7189
E-mail: info@ligo.caltech.edu

http://www.ligo.caltech.edu/

1 Introduction and Motivation

The Advanced LIGO interferometers are among the most sensitive instruments ever constructed. Even as these observatories progress towards achieving their design sensitivity, work is under way in planning even more sensitive successors [1][2][3]. These will incorporate the the state of the art in materials, control and sensing technology. Key to reaching these improved design sensitivities will be the implementation of cryogenic test masses[1]. These will likely be made from crystalline silicon and will be probed with longer wavelengths in the range of 1550-2000 nm. The choice of $2\mu m$ laser light is a strong candidate wave length given the transparency window of the materials and reduced scatter[4]. Less well known is the performance limitations of lasers of this type and how they might be pre-stablized for use in demanding interferometric experiments.

While NPRO style lasers, previously used at 1064 nm in LIGO, offered inherently narrow line width light, newer fiber coupled technologies such as Discrete-Mode diode lasers are now commercial available at competitive prices. Direct stabilization of these seed laser sources using all fiber assemblies may offer a compact, affordable and low maintenance alternative to more traditional reference cavity pre-stabilization schemes. The characterization of an all fiber stabilized diode laser source will be an important step for delivering $2\mu m$ light to table top experiments used in testing various $2\mu m$ devices for future LIGO use. It will also be an important first step for building a test-bed for assessing the goodness of candidate laser sources for future long wavelength laser interferometers.

Laser stabilization is important for reducing frequency and intensity noise in optic systems. In a system involving a single-frequency laser, there is always noise associated with its output, causing its monochromatic nature to be broadened in its spectral output. Noise in laser sources can originate from a multitude of sources including external acoustic disturbances, internal thermal drift, and spontaneous emission within the laser's gain medium(i.e. quantum noise). Understanding and accounting for these sources is a crucial aspect in obtaining a low noise light source for interferometric experiments. Current LIGO technology uses a 125W laser of 1064nm light and one of the modifications for the LIGO Voyager upgrade is a longer wavelength laser of 2004nm. (This experiment aims to demonstrate all fiber optic stabilization of a relatively noisy (2 MHz linewidth) diode laser source and establish performance limits of such as simple system.)

2 Objectives

The goal of this all-fibered Mach-Zehnder intereferometer(shown in Figure 1) project is to actively stabilize a 2 μm laser and characterize both its *frequency* and *intensity* noise. We will use a path length difference in the intereferometer to make a frequency discriminator and an InGaAs photodiode to measure intensity noise. This project is motivated by the current stage in the LIGO3 PSL Timeline, Noise Characterization and Long-term Stability[1].

To achieve this objective, we will employ a closed loop feedback control system in our set-up to stabilize the frequency of our laser under test. Additionally, we will design an encasement around our intereferometer to passively supress as much thermal and acoustic perturbations

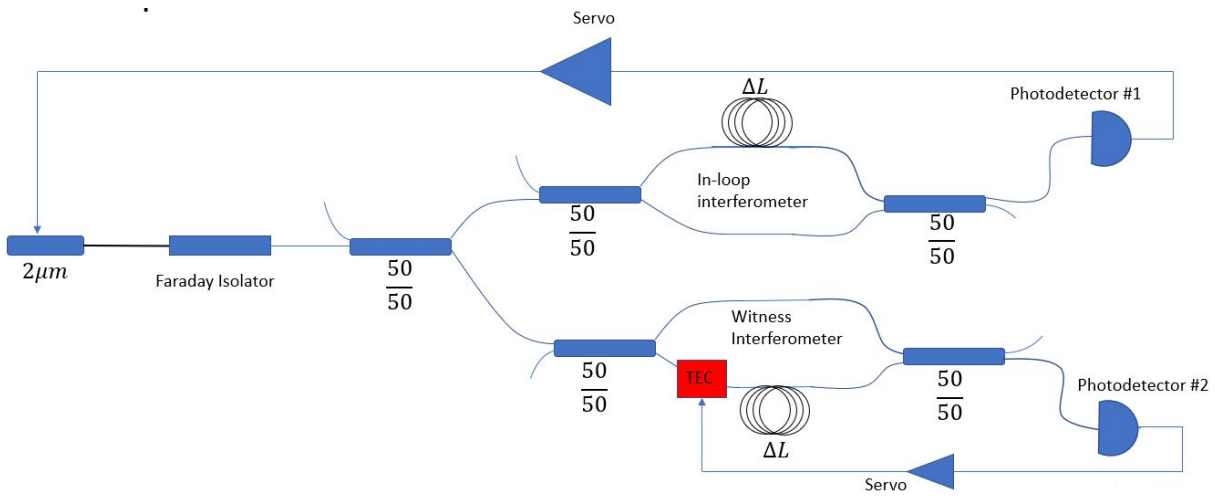

Figure 1: *Experiment set-up, with Mach-Zehnder interferometer delay line and its reference*

as possible. Depending on the progress of the project, we will conclude by investigating the usage of an acousto-optic modulator for intensity noise stabilization. The ideal conclusion of our experiment would be additional data that can support the usage of a longer wavelength laser on the new generation LIGO Voyager.

3 Experimental Set-up

3.1 Experiment Housing

To avoid undesired disturbances that could affect our measurements, we housed our experiment in a 17.5x25.5x60.5cm metallic casing with a plexiglass lid. The inner walls are covered with noise-insulating foam padding, as is the table top surface upon which the experiment lies. With the encasing set up, we noticed a decrease in the swaying of the intensity in our measurements of the photodetector's power output.

3.2 Optical Components

To have a better understanding of the limitations through our optical components, we measured the power losses through each of them. As expected, particularly in the case of the beam splitters, there are deviations from their 50/50 nature.

We can determine the excess power loss, L_p, by considering the total output power from the laser, and the outputs from both ends of the beam splitter under analysis. The following expression is observed:

$$L_p = 10 \log \frac{P_{in}}{P_1 + P_2} \tag{1}$$

The output power measured at different locations throughout the experiment are shown

below.

Stage-by-stage Power Output		
From Laser through ...	Power (mW) (+/- 0.002mW)	Power Loss (dB)
Directly from laser	1.339	-
Faraday Isolator	0.894	-
Pre-loop Beam Splitter, Short arm	0.528	0.351
Pre-loop Beam Splitter, Long arm	0.707	0.351
After Longer arm	1.291	-
Post-loop Beam splitter (to Photodiode)	0.762	0.327
Post-loop Beam Splitter (to Beam dump)	0.480	0.327

3.3 Interferometers

Both the witness and reference interferometers incorporate in their delay lines the ThorLabs SM2000 Ge-doped-silica-core optical fiber with a cutoff wavelength at around 1750nm and an operational limit of 2300nm. For our usage at $2\mu m$, the fiber has an attenuation of 37 dB/km [12]. An all fiber set-up offers a number of advantages over equivalent free-space configurations. Prototyping and field deployment are aided by ease of construction with robust alignment free connections as well as compact implementation of long delay lines.

4 Delay Line

4.1 Frequency Noise

The highly coherent light from our laser under test will necessarily have some associated frequency and amplitude noise. Frequency noise can be described as the random fluctuations in the frequency of some oscillating signal. For our experiment we characterize it as an ASD spectrum. The frequency noise can be expressed as the temporal derivative of that oscillating phase:

$$\nu(t) = \frac{\Delta\phi}{2\pi\Delta t} \tag{2}$$

$$\Delta\phi = 2\pi(\frac{n\Delta L}{c})\nu(t) \tag{3}$$

Where $\Delta\phi$ is is change in phase, ΔL the path length mismatch, and n the refractive index of the optical fiber.

4.2 Optimal Path Length

Due to the presence of a delay-line in our interferometer, one of the most pressing challenges we initially faced was to calculate the optimal optic fiber length for the arm mismatch. There are various factors that contribute to finding the optimal fiber length such as the power loss throughout the fiber, thermo-optic noise (manifested through the temperature dependance of the fiber's refractive index and linear thermal expansion coefficient), and the fiber's acoustic sensitivity. The underlying matter of this challenge is determining the sensitivity of our interferometer, taking into account the balances between cost and sensitivity losses.

To have a better sense of the ideal sensitivity of our interferometer, we needed to further elaborate on the rough noise budget we had created before the start of the project. With a smaller version (i.e. an interferometer with a shorter length mismatch than desired) of the project already set up, we have begun gathering noise data on the various components used in the set-up, such as our DET10D Photodiode, any required op-amp circuits that we build, and the 2 micron laser itself. Some sources of noise were acquired through manufacturer documentation and simply converted into the equivalent frequency noise (Hz/rtHz), to be added onto our noise budget.

We began with the power loss versus fiber length optimization by considering power at one of our interferometer's outputs, with an attenuation coefficient, α. In the following expression of output power, P_{in} represents in the input power, L_1 and L_2 represent the length of arm 1 and 2 of the interferometer, and ΔL represents the path length mismatch between the arms.

$$P_{out} = \frac{P_{in}}{4}(e^{-2\alpha L_1} + e^{-2\alpha L_2} + 2\cos(\frac{2\pi f\Delta L}{c})e^{-2\alpha(L_1+L_2)}) \tag{4}$$

Shown in Figure 2, the rate change of the output power with respect to the frequency can then be expressed as,

$$\frac{\delta P_{out}}{\delta f} = \frac{P_{in}}{4}(e^{-2L_1\alpha} + e^{-2L_2\alpha}) \tag{5}$$

Since the ideal scenario for our experiment is to lock the laser's frequency at mid-fringe, we must find where the slope of the output power with respect to the laser's frequency ($\frac{\delta P_{out}}{\delta f}$) is greatest. Taking another derivative of this expression with respect to the long arm length L_2 provides us the sensitivity (S_i) slope of the optic fiber:

$$S_i = \frac{-e^{-\alpha(L_1+L_2)}\pi P_{in}}{c} + \frac{e^{-\alpha(L_1+L_2)}\pi\alpha\Delta L P_{in}}{c} \tag{6}$$

The attenuation coefficient was found by referring to the spec sheet of the desired SM2000

Ge-doped optical fiber by ThorLabs [12]. At a wavelength of 2004nm, the attenuation is given to be roughly $37.5 * 10^{-3} dB/km$. Finding α is as follows, where β is the given attenuation:

$$\alpha = \frac{\beta}{\log e} \tag{7}$$

With the attenuation coefficient of $8.63 * 10^{-3}/m$, the plot of $\frac{\delta P_{out}^2}{\delta^2 f}$ is shown in Figure 3. Even with a 10 percent sensitivity range reduction, the optimal path length would be around 57.9 meters. Thus, the tested length of 10m is adequate for an initial prototype.

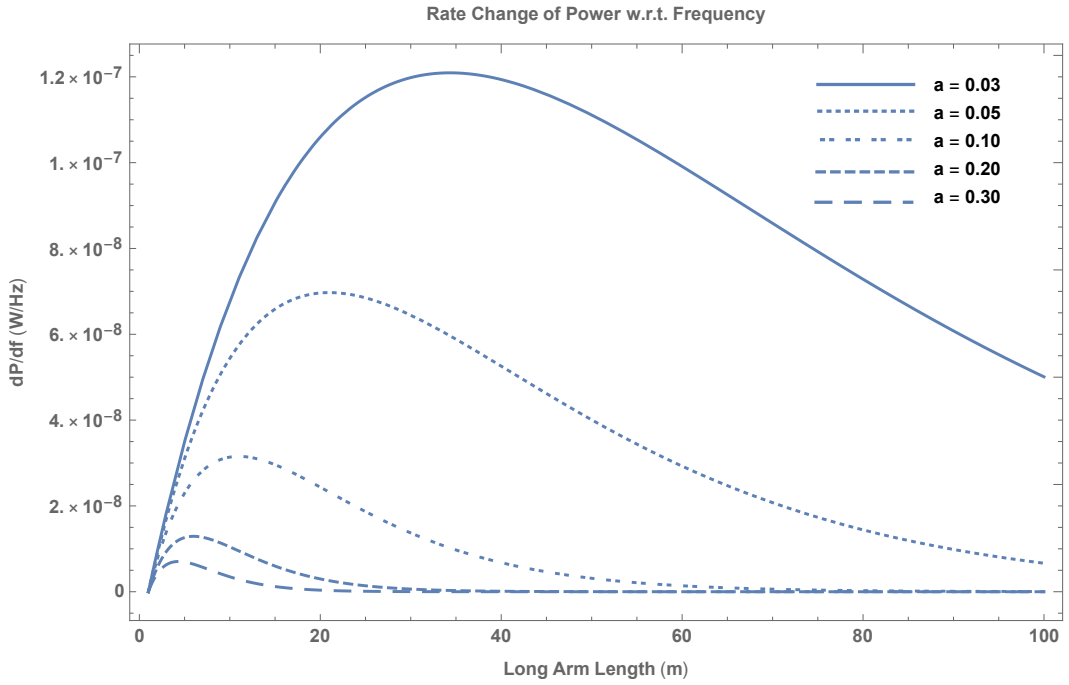

Figure 2: *The rate change of the photodiode output power with respect to frequency at selected attenuation constants.*

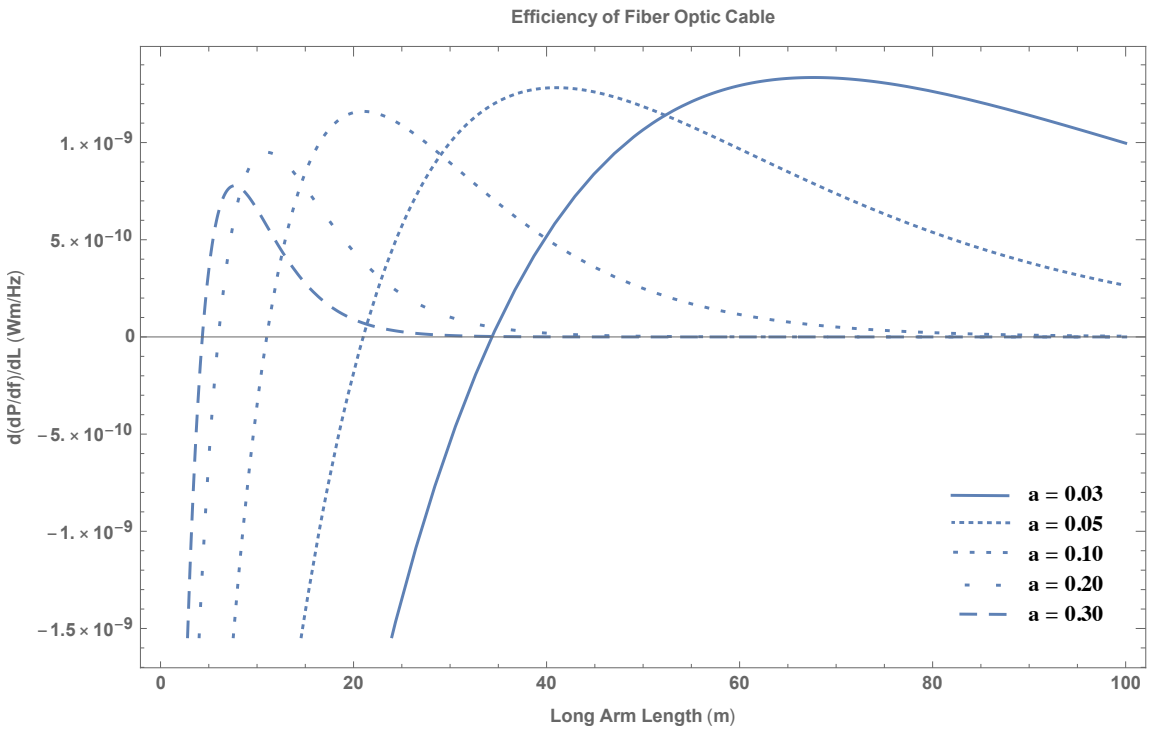

Figure 3: *The sensitivity slope of the fiber optic cable as a function of the long arm length, L_2. The zero points correspond to the ideal length given some attenuation constant.*

The experiment currently has a 10 meter path length difference, which should provide an increase of fringe visibility while not exceedingly suffering the effects of the inherent power loss associated with longer lengths.

5 Closed Feedback Loop

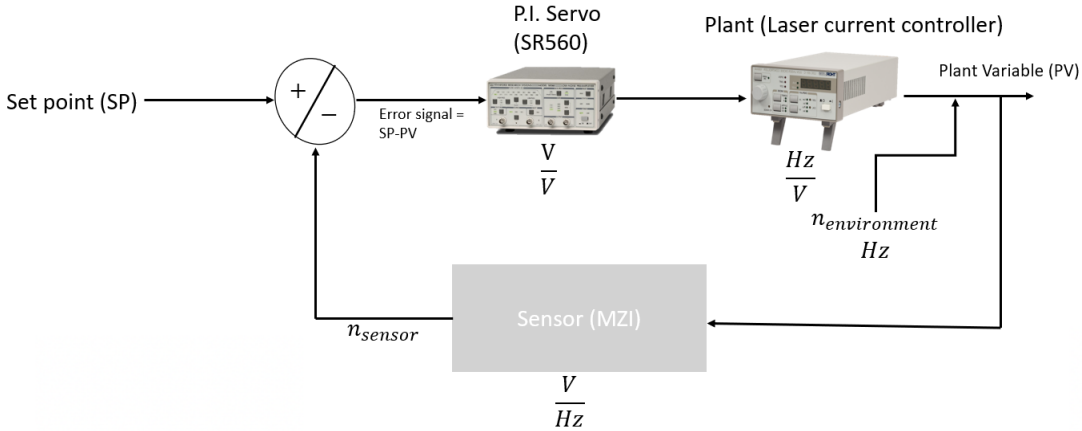

Figure 4: *Control loop diagram overview of the TMTF.*

6 Noise Budget

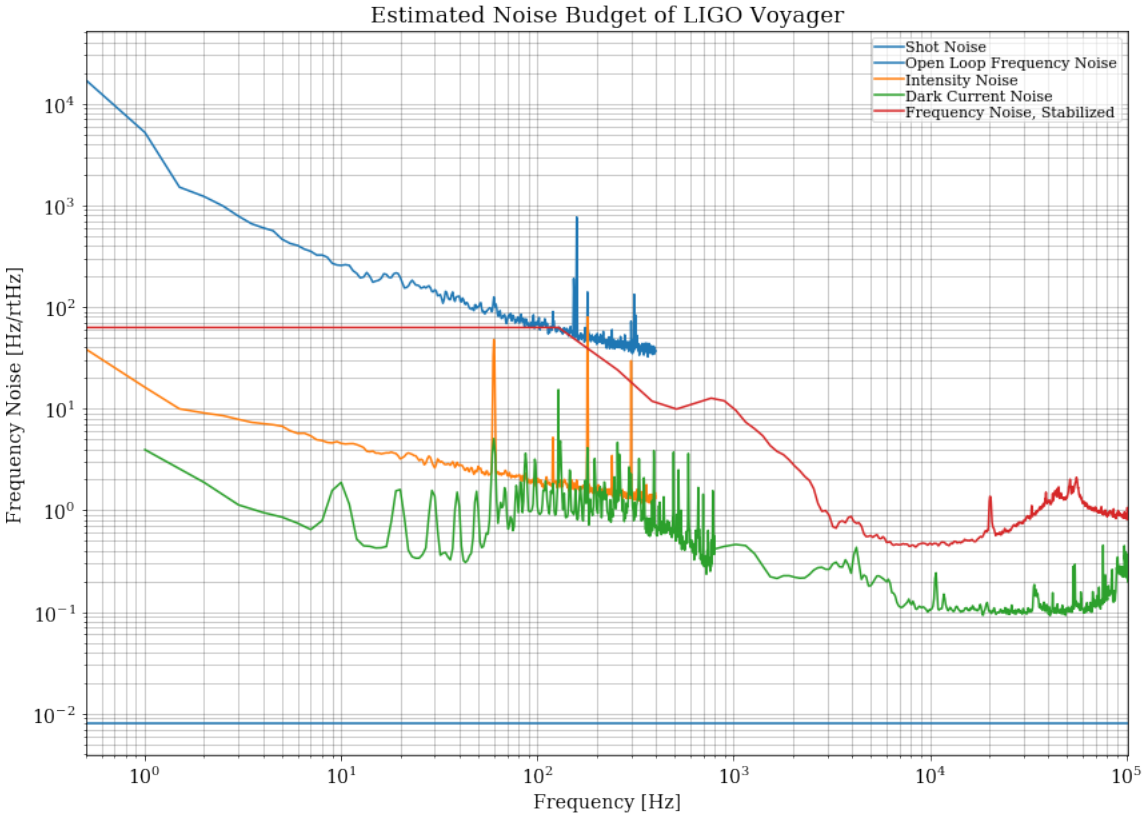

Figure 5: **Noise Budget for 2μm Experiment**, *Shown are the amplitude spectral density of the frequency noise of various sources in the overall set-up. Together they contribute into our system's noise budget, and are compared with the estimated frequency noise requirement of the Voyager 2μm laser, shown with the black line, which itself comes from the 1kHz linewidth NPRO frequency noise spectrum scaled by 2000. Based on the laser's wavelength and input power, the shot noise was calculated to be* $2.276 \times 10^{-11}\,\mathrm{W/Hz^{1/2}}$. *From manufacture documentation, the value of the photodiode NEP is* $1.50 \times 10^{-12}\,\mathrm{W/Hz^{1/2}}$. *Assuming a 15m arm length mismatch, the frequency noise equivalent power was calculated to be* $8.144 \times 10^{-3}\,\mathrm{Hz/Hz^{1/2}}$ *and* $5.358 \times 10^{-4}\,\mathrm{Hz/Hz^{1/2}}$ *for the shot noise and photodiode respectively.*

6.1 Detector Dark Noise

Dark noise is a current leakage characteristic shared by diodes and arises when a biased voltage is applied in the detector. Upon measuring the dark noise from our DET10D photodiode, we came across the issue that the photodiode was DC biased. This prompted us to develop a simple transimpedance op-amp with the purpose of providing an optimal reading scheme for our measuring instrument and a better signal-to-noise ratio where only the photodiode's shot noise would be the circuit's limiting factor. The schematic is shown in Figure 6. We ran into difficulties in measuring the output signal from the circuit due to a reoccuring oscillations. These oscillations are present due to the large phase margin for the product between the op-amp's gain and feedback factor.

Essentially, this is an op-amp phenomena where instability occurs if the rate of the closure between the curves of the gain and reciprocal of the feedback factor approach $40dB$ per decade.

6.2 Shot Noise

The shot noise of a photodetector describes its optical intensity noise limit and arises from the discrete nature of electrons and photons, and is a property of a light field[7]. The shot noise of our photodiode can be expressed by the following relationship:

$$\delta n_{sn} = \sqrt{2e^{-}\bar{I}}$$

Where $\bar{I}$ is the average current through the photodiode; gathered from the product of the photodiode's responsivity, approximately $1.2A/W$, and the current reaching the photodiode in our interferometer which we estimate to be roughly $100\mu W$[8]. With this information, it's possible to reach a figure of $6.2 * 10^{-12}A$ for $\bar{I}$. Thus, the shot noise we expect to observe from our photodiode is $6.2 * 10^{-12}A$. Fortunately, the input referred current for the OP27 ,$0.4\frac{fA}{\sqrt{Hz}}$ at $1kHz$, is lower than this threshold.

6.3 Photodetector Modifcations

Our primary modification to the photodetector was the addition of a transimpedance amplifier (TIA), used for high impedance voltage signal conditioning. The motivation behind this was to improve the signal-to-noise ratio of the output signal and widen the bandwidth of the of the detector response. To stabilize our TIA, we added a 200pF phase compensator to the circuit's architecture. Shown below is the schematic for the TIA in the the TMTF.

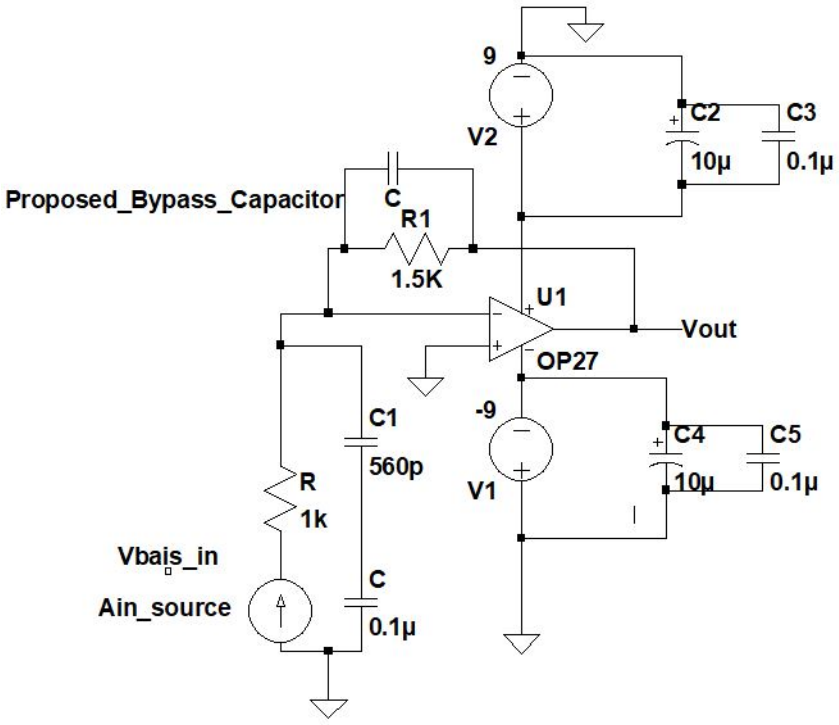

Figure 6: *Schematic for transimpedance op-amp used in conjuction with DET10D photodiode.*

6.4 Acoustic and Thermal Sensitivity

We predict that acoustic noise will be a limiting noise factor in our experiment at lower frequencies, thus having a grounded notion of the sensitivity of our optic fiber is crucial when considering a possible length to purchase. The fiber's sensitivity to some pressure depends on its characteristic elastic coefficients (Young's Modulus, E, and Poisson's Ratio, σ) and Pockels coefficients, P_{12} and P_{44} [9]. Previous work has been done to calculate these coefficients for pure silica, the material found within the core and part of the cladding of our optic fiber. In an idealized state, our optic fiber can be treated as a cylinder of pure silica. Referenced work measured the pressure acting on the material from variations of the relative phase change between two interferometer arms- one static and the other undergoing a pressure difference relative to it. The optical phase retardation per unit of pressure can be expressed as,

$$\frac{\Delta\phi}{\phi} = \frac{(1-2\sigma)}{E}(\frac{n^2}{2}(3P_{12}+2P_{44}))$$

Following this idealized scenario, the acoustic sensitivity comes out to be $-1.23{*}10^{-14} dyn/cm^2$. We are currently reviewing the scientific precedence on calculating the acoustic sensitivity of a multilayered "cylinder", essentially replicating our optic fiber, which takes into account the varying refractive indices and radial/axial strains[10].

7 Stabilization

The process of locking and stabilizing the $2\mu m$ laser involves setting up the experiment as a closed feedback loop, shown in Figure **??**. Upon first measurement of the photodetector signal with the laser off, we noticed a DC offset of about 22.4×10^{-3} V, whose cause we are still determining. The next steps take into account this offset. The next step involves finding the mid-fringe point of the photodetector output with the laser turned on, which we determined to be 440×10^{-3} V above the offset. We then subtract a voltage reference with an identical value from the PD output to produce an error signal, which is subsequently fed back to the laser diode's current controller, completing the feedback loop. We utillize two daisy-chained pre-amplifiers as the gain element in the feedback loop, with one having a high-pass filter of 1 Hz and 6 dB rolloff and the other DC coupled. Upon DC coupling the two pre-amplifiers and increasing the gain, we expected a linearization of the error signal but instead observed it scanning through a large quantity of fringes, which also caused the laser diode current controller to drastically fluctuate in current value. These characteristics indicate an imperfection in the feedback loop architecture.

Adjusting for these imperfections by rearranging the directions of the optic fiber and increasing the gain in our pre-amplifier to 10x, we observed a more stable regime, shown in Figure 7. A spectral analysis of the experiment in this state results in the following figure, 8.

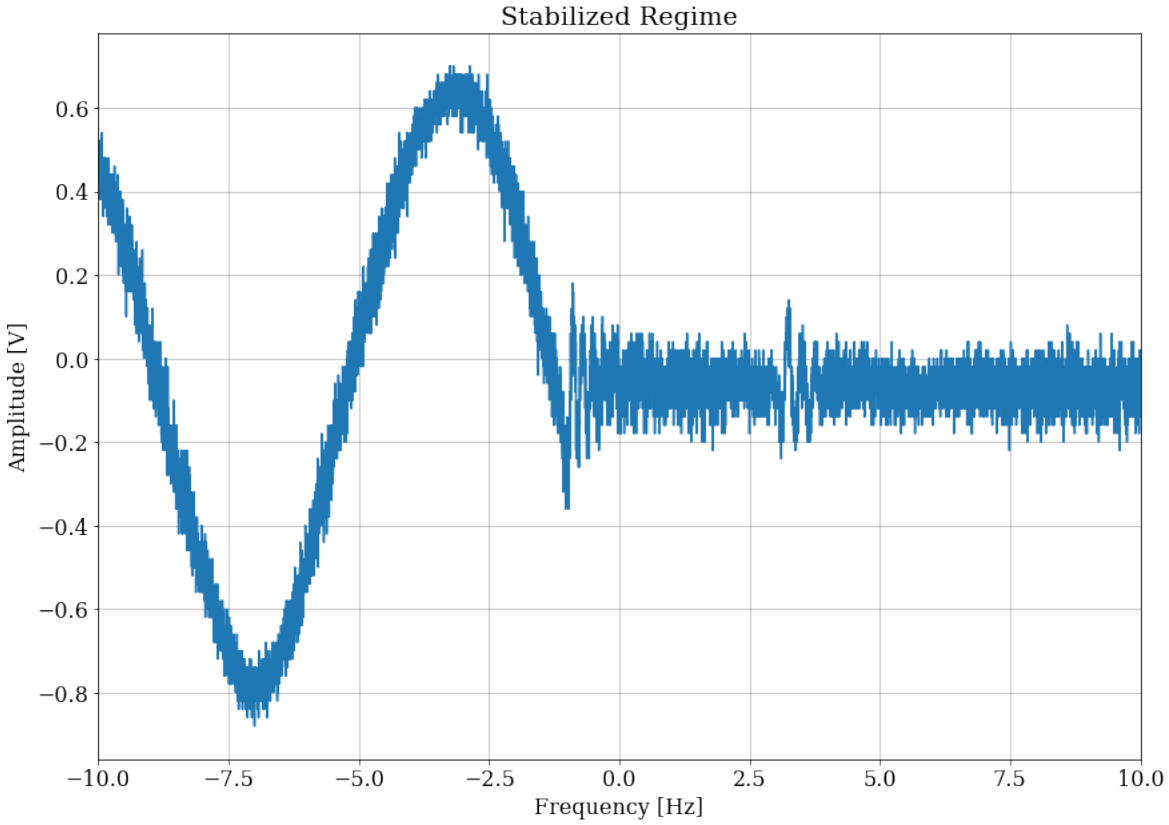

Figure 7: **Spectrum Analysis of the Two Micron Test Facility**, *Shown are the ASD's of the frequency noise in both a stabilized regime and open loop feedback.*

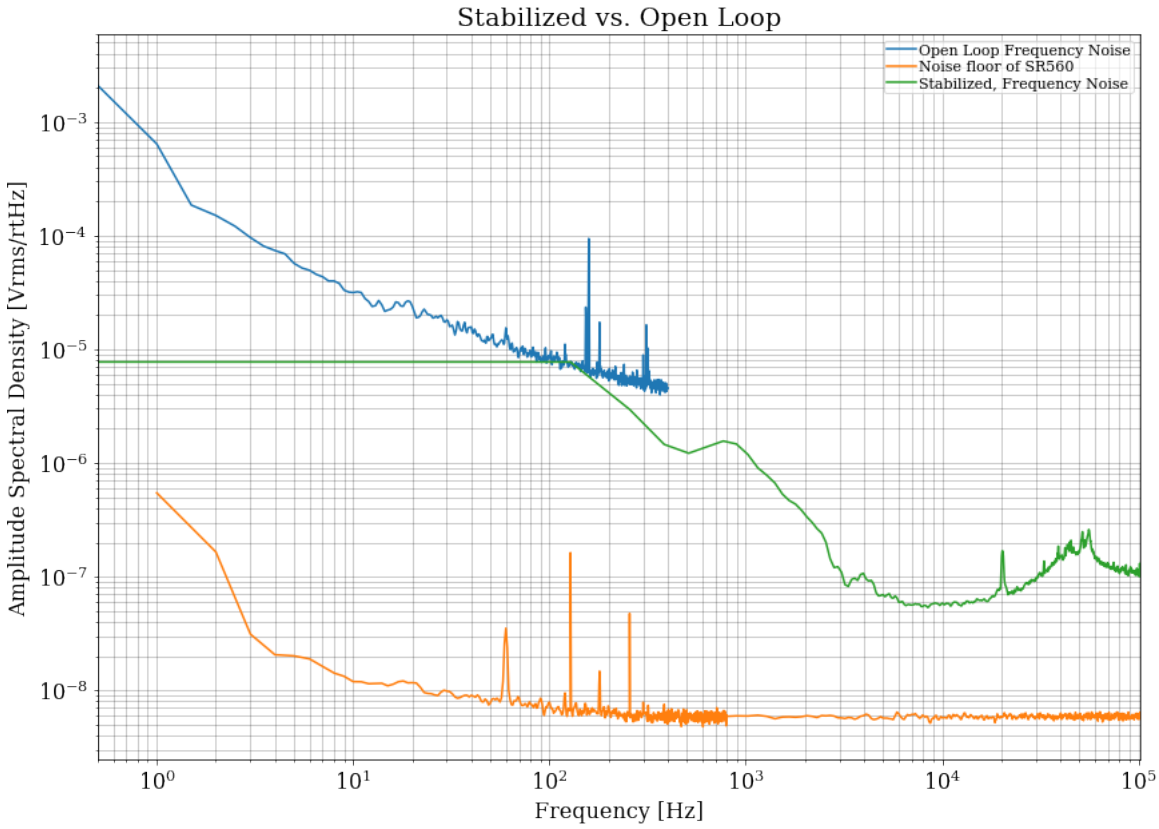

Figure 8: **Spectrum Analysis of the Two Micron Test Facility**, *Shown are the ASD's of the frequency noise in both a stabilized regime and open loop feedback.*

8 Conclusions

In our current set-up, we achieved stabilization, although the sensitivity reached in our experiment fell roughly 2 orders of magnitude above the predicted LIGO Voyager requirements, with 50 $\mathrm{Hz/Hz^{1/2}}$ at 1000 Hz, the overall pathway is set in place for optimizations. The most immediate task with which to follow-up is the sensitivity measurement of the TEC-actuated witness interferometer.

9 Future Work

A possible and practical line of experimentation would be to alter the optic fiber paths into a Michelson Inteferometer format, using 3x3 optic coupling. A previous experiment in this style showed promising results in the characterization of a semiconductor laser[11]. Additionally, the thermal sensors that have been built can be utilized within and and around the experiment to capture temperature drifts which could add unwanted drift to our experiment's output. Since measuring the inherent acoustic sensitivity of the experiment's optical fibers material may prove to extend passed the reach of our schedule, a viable route for experimentation would be the addition of a microphone along with a piezo-buzzer within

the housing of the experiment. This would allow us to experimentally measure the degree of sensitivity of the optical fiber, when compared to a normal lab volume conditions.

Finally, the continuation of the project would include characterizing the sources of noise found within the ASD analysis.

10 Acknowledgments

An immense thanks to Andrew Wade and Aidan Brookes for their mentorship throughout this project, as well as the Caltech LIGO SURF program for access to the facilities in which the experiment took place. A special thanks to Alan Weinstein for bringing the 2018 Summer SURF program together.

References

[1] Adhikari, Rana X, et. al, *LIGO Voyager Upgrade: Design Concept*. LIGO Scientific Collaboration, LIGO-T1400226-v9 (2014)

[2] Hild, Stefan, et. al, *Pushing towards the ET sensitivity using "conventional" technology*. School of Physics and Astronomy at University of Birmingham, Issue 2 (2014)

[3] LIGO Scientific Collaboration, *Instrument Science White Paper*. LIGO Scientific Collaboration, LIGO-T15TBIv1 (2014)

[4] Edward, Taylor and Smith-Lefebvre, Nicolas, *Quality Factor of Crystalline Silicon at Cryogenic Temperatures*. LIGO Scientific Collaboration (2013)

[5] Conant, Emily; Hall, Evan; Adhikari, Rana; Chalermsongsak, Tara, *Transportation of Ultra-Stable Light via Optical Fiber*. LIGO Scientific Collaboration, T1400501-v1 (2014)

[6] Callen B., Herbert and Welton A., Theodore, *Irreversibility and Generalized Noise*. Randal Morgan Laboratory of Physics, University of Pennsylvania (1951)

[7] Richardson, W. H., et. al, *Squeezed Photon-Number Noise and Sub-Poissonian Electrical Partition Noise in a Semiconductor Laser*. NTT Basic Research Laboratories(1991)

[8] ThorLabs, *DET10D(/M) Extended InGaAs Biased Detector, User Guide* (2017)

[9] N. Lagakos, et. al, *Acoustic sensitivity predictions of single-mode optical fibers using Brillouin scattering*. Applied Optics, Vol. 19, No. 21 (1980)

[10] Hughes, R. and Jarzynski, J., *Static pressure sensitivity amplification in interferometric fiber-optic hydrophones*. Applied Optics, Vol. 19, No. 21 (1980)

[11] Xu, Dan, et. al., *Laser phase and frequency noise measurement by Michelson interferometer composed of a 3 3 optical fiber coupler*. Optics Express, Vol. 23, No. 17 (2015)

[12] ThorLabs, *SM2000 Specifications Sheet, https://www.thorlabs.com/drawings /SM2000-SpecSheet.pdf* (2015)